



King Saud University  
Arabian Journal of Chemistry

www.ksu.edu.sa  
www.sciencedirect.com



## ORIGINAL ARTICLE

# Preparation and characterization of mesoporous activated carbons from waste watermelon rind by using the chemical activation method with zinc chloride

Osman Üner<sup>a,\*</sup>, Ünal Geçgel<sup>b</sup>, Yüksel Bayrak<sup>c</sup>

<sup>a</sup> Department of Chemistry, Kırklareli University, 39020 Kırklareli, Turkey

<sup>b</sup> Arda Vocational College, Trakya University, 22030 Edirne, Turkey

<sup>c</sup> Department of Chemistry, Trakya University, 22030 Edirne, Turkey

Received 3 October 2015; accepted 2 December 2015

## KEYWORDS

Waste watermelon rind;  
Activated carbon;  
Chemical activation;  
Zinc chloride;  
Pore property

**Abstract** Waste watermelon rind was analyzed as a precursor for preparing activated carbons by using a one-step chemical activation process by zinc chloride. The effects of activation parameters, i.e., carbonization temperature, impregnation ratio, and impregnation time on the properties of the final products were tested in detail. The resultant activated carbons were characterized using elemental analysis, the Brunauer–Emmet–Teller method, pore property analysis, N<sub>2</sub> adsorption/desorption isotherms, Fourier transform infrared spectroscopy, the point of zero charge, Boehm titration method and scanning electron microscopy. The maximal Brunauer–Emmett–Teller surface area of the resultant activated carbon, produced by using the impregnation (ZnCl<sub>2</sub>/dried watermelon rind) ratio of 2/1 at the carbonization temperature of 700 °C with the residence time of 60 min, was 1156 m<sup>2</sup>/g. Upon using the impregnation ratio of 3/1 at the carbonization temperature of 600 °C with the residence time of 60 min, the maximal total pore volume, which also contains the highest mesopore volume, was 1.41 cm<sup>3</sup>/g.

© 2015 The Authors. Production and hosting by Elsevier B.V. on behalf of King Saud University. This is an open access article under the CC BY-NC-ND license (<http://creativecommons.org/licenses/by-nc-nd/4.0/>).

\* Corresponding author. Tel.: +90 (288) 246 17 34; fax: +90 (288) 246 17 33.

E-mail addresses: [osmanuner@klu.edu.tr](mailto:osmanuner@klu.edu.tr) (O. Üner), [unalgecgel@trakya.edu.tr](mailto:unalgecgel@trakya.edu.tr) (Ü. Geçgel), [yukselbayrak@trakya.edu.tr](mailto:yukselbayrak@trakya.edu.tr) (Y. Bayrak).

Peer review under responsibility of King Saud University.



Production and hosting by Elsevier

## 1. Introduction

Producing activated carbon (AC) from waste biomass has become popular because of its low cost and efficiency mainly in adsorption processes to remove toxic materials from aqueous solution (Yahya et al., 2015). Activated carbon is an amorphous carbon material characterized by its surface chemistry and textural properties, i.e., surface area and porosity. These AC properties strongly depend on the starting material and its preparation process. A variety of waste biomaterials with high carbon content are widely used as starting materials for

<http://dx.doi.org/10.1016/j.arabjc.2015.12.004>

1878-5352 © 2015 The Authors. Production and hosting by Elsevier B.V. on behalf of King Saud University.

This is an open access article under the CC BY-NC-ND license (<http://creativecommons.org/licenses/by-nc-nd/4.0/>).

Please cite this article in press as: Üner, O. et al., Preparation and characterization of mesoporous activated carbons from waste watermelon rind by using the chemical activation method with zinc chloride. Arabian Journal of Chemistry (2015), <http://dx.doi.org/10.1016/j.arabjc.2015.12.004>

obtaining ACs, such as coconut shells (Daud and Ali, 2004), almond shell and walnut shell (Gonzalez et al., 2009), rice stalk (Ai et al., 2013), pine sawdust (Açıkyıldız et al., 2014), and orange peel (Köseoğlu and Akmil-Başar, 2015). Recently, activated carbons with very high surface area have been obtained by chemical activation, and activated carbons prepared from waste biomaterials through the chemical activation method have been extensively used for the removal of pollutants (Hayashi et al., 2000; Açıkyıldız et al., 2014; Okman et al., 2014; Qin et al., 2014; Yagub et al., 2014; Yahya et al., 2015; Saygılı et al., 2015).

At chemical activation processes, well-known chemical agents, i.e.,  $ZnCl_2$ ,  $H_3PO_4$ ,  $H_2SO_4$ ,  $K_2S$ ,  $KCNS$ ,  $HNO_3$ ,  $H_2O_2$ ,  $KMnO_4$ ,  $(NH_4)_2S_2O_8$ ,  $NaOH$ ,  $KOH$  and  $K_2CO_3$  are used to activate carbons, resulting in a high surface area and appropriate porous structure (Yahya et al., 2015). Among these chemical activating agents,  $ZnCl_2$  is widely preferred, because it is efficient in producing a greater surface area (Donald et al., 2011). Activated carbons with high micropore volume are widely used for the adsorption of small sized molecules, but adsorbents with high mesopore volume are required for the adsorption of large molecules, such as dyes and compounds with high molecular weights. Therefore, carbons with high mesopore volume are utilized in numerous applications, such as in lithium batteries (Ryoo et al., 2001), electro-catalysis (Calvillo et al., 2007), the removal of dyes from aqueous solution (Zhuang et al., 2009), biocatalysis (Talapaneni et al., 2012), and electrochemical capacitors (Dai et al., 2014).

Waste watermelon rind, a waste biomaterial, has not yet been evaluated as a raw material for the production of activated carbon using the chemical activation method by zinc chloride. Thus, the main objective of the present work was to evaluate the utility of waste watermelon rind as an abundant and accessible precursor for activated carbon production. The influences of impregnation ratio, carbonization temperature, and carbonization time on WAC characteristics were investigated. Moreover, elemental analysis,  $N_2$  adsorption/desorption isotherms, Fourier transform infrared spectroscopy (FTIR), the point of zero charge ( $pH_{pzc}$ ), Boehm titration, and scanning electron microscopy (SEM) were performed for better WAC characterization.

## 2. Materials and methods

### 2.1. Materials

Watermelon rind used in this study was obtained from a local market in Edirne, Turkey. Watermelon rind was washed with double distilled water and placed in a blender with electromechanical controls to break into small pieces. The watermelon rinds broken into small pieces were left under the sun for two days on the summer days to evaporate their water. Then, dried watermelon rinds (dWRs) were milled to be smaller than 50 mesh, and stored in brown glass bottles.  $ZnCl_2$  and  $HCl$  were obtained from Merck. Sodium hydroxide, sodium carbonate, and sodium bicarbonate were obtained from Sigma–Aldrich.

### 2.2. Preparation of activated carbon

Five grams of dWR were inserted into each of five flasks, and  $ZnCl_2$  solutions whose impregnation ratios ( $ZnCl_2$ /dWR) were 0.5/1, 1/1, 2/1, 3/1 ve 4/1 (w/w) were added to these flasks in order to activate the carbons. The mixtures in the flasks were refluxed below their boiling points for an hour and then dried in petri dishes in an incubator for 24 h at 105 °C. After drying, the carbonizations of the mixtures were completed by baking in a furnace (nüve, MF 120) at different temperatures,

i.e., 400, 500, 600, 700 and 800 °C for 30, 60, 90 and 120 min. separately. The obtained watermelon activated carbons (WACs) were treated with 0.1 N  $HCl$  solutions, and then washed with double distilled water until neutral pH was attained. After an additional drying step in the incubator at 105 °C, the WACs were ground and stored for future use.

### 2.3. Characterization techniques

Elemental contents (C, H, N, S) of dWR and WAC at 600 and 700 °C were obtained using an elemental analyzer (Leco TrueSpec Micro). Oxygen content was calculated from the difference. The surface areas and pore volumes were carried out by measuring  $N_2$  adsorption–desorption isotherms at liquid nitrogen temperature (–196 °C) on an automatic apparatus (Micromeritics TriStar II 3020) after degassing the carbon samples sequentially at 105 °C for 30 min and at 300 °C for 120 min. under  $N_2$  atmosphere to remove volatile contaminations. The surface areas of WACs with different impregnation ratios, carbonization temperatures, and carbonization times were calculated by applying the Brunauer–Emmett–Teller (BET) model (Lowell and Shields, 1991) to the isotherm data of the adsorption branch in the relative pressure range  $p/p_0 < 0.21$ . The total pore volumes were obtained at a relative pressure of about 0.98, and micropore surface areas and micropore volumes were estimated using *t*-plot method (Lowell and Shields, 1991). The mesopore areas and the mesopore volumes were calculated by subtracting the micropore values from the total values.

FTIR spectroscopy (Perkin Elmer, FT-IR/FIR Spectrometer Frontier) was used to determine the functional groups present in dWR and WAC. The point of zero charge was measured to obtain information of the surface charge on WAC via a batch equilibrium procedure (Milonjić et al., 1975). This measurement was carried out as follows: 50 mL of  $KNO_3$  solution (0.1 M) was placed in an Erlenmeyer flask including 0.1 g of WAC. The initial pH was adjusted between 2 and 12 by addition of  $NaOH$  or  $HCl$  (0.1 N). After a contact time of 48 h under magnetic agitation at 150 rpm, the ultimate pH was determined and plotted versus the initial pH.

The surface functional groups containing oxygen were determined using Boehm titration (Boehm, 1966, 1994). WACs of 0.5 g were separately placed in 50 mL of the following solutions of 0.05 N: sodium hydroxide, sodium carbonate, sodium bicarbonate, and hydrochloric acid. The vials were sealed and agitated for 24 h and then filtered. 10.00 mL aliquots were taken.  $NaHCO_3$  and  $NaOH$  samples were acidified with the addition of 20.00 mL standardized 0.05 N  $HCl$ , while for  $Na_2CO_3$ , 30.00 mL of 0.05 N  $HCl$  was added to neutralize the diprotic base completely and then allowed a strong acid–strong base titration. The excess base or acid was titrated with standardized 0.05 N  $HCl$  or  $NaOH$ , respectively. The number of acidic sites was found under following assumptions.  $NaOH$  neutralizes carboxylic, lactonic, and phenolic groups.  $Na_2CO_3$  neutralizes carboxylic and lactonic groups.  $NaHCO_3$  neutralizes only carboxylic groups. Also, the number of basic sites was calculated from the amount of hydrochloric acid that reacted with WAC. Furthermore, dWR and WAC were analyzed using a scanning electron microscopy (SEM; FEI-QUANTA FEG 250) to observe the variations on the surface morphologies.

### 3. Results and discussions

As seen in Table 1, the surface areas of all WACs whose carbonization processes were carried out at 400–800 °C for 30, 90, and 120 min. were determined to be below 300 m<sup>2</sup>/g. This can explain that the carbonization time of 30 min. is not sufficient to form porous structures on WAC, and some dried watermelon stayed as uncarbonized. On the other hand, the surface areas of WACs had low values when carbonization processes were performed at 400–800 °C for 90 and 120 min. because more time for carbonization process may affect surface area adversely by disrupting the surface structure of WACs. Therefore, WACs whose carbonization processes were completed at 400–800 °C for 60 min were investigated in detail.

#### 3.1. Elemental analyses

Elemental compositions of dWR and WACs carbonized at 400–800 °C are given in Table 2. The carbon content of WAC substantially increased compared to dWR after activation process. Hydrogen and oxygen contents showed the opposite change trend as expected. Because of dWR decomposition in the activation and carbonization processes, volatile compounds, such as hydrogen and oxygen left the carbonaceous product. Therefore, the carbonaceous product became rich in carbon.

#### 3.2. Influence of chemical impregnation ratio and temperature on the surface area

The surface areas of WACs prepared at different temperatures and different impregnation ratios are shown in Fig. 1. As the

**Table 2** Elemental contents (% w/w) of dWR and WACs with impregnation ratio of 2/1.

Sample	C	H	N	S	O (diff.)
dWR	38.57	5.94	2.60	0.97	51.92
WAC-400	44.15	4.54	3.17	1.14	47.00
WAC-500	49.74	3.29	3.95	1.19	41.83
WAC-600	54.38	1.77	4.72	1.21	37.92
WAC-700	60.42	1.54	4.47	1.68	31.89
WAC-800	47.25	3.84	3.74	1.17	44.00

carbonization temperature increases from 400 to 700 °C, the surface area of WAC increases, but increasing temperature from 700 to 800 °C causes to decrease the surface area of WAC dramatically. It is observed that the surface areas of WACs are below 800 m<sup>2</sup>/g when the carbonization processes are completed at 400, 500, and 800 °C. The surface areas of WACs carbonized at 600 and 700 °C are much larger than the others. One of the other parameters affecting the surface areas is impregnation ratio shown in Fig 1. For all carbonization temperatures, as the impregnation ratio increases from 0.5 to 2, the surface area of WAC increases, but increasing impregnation ratio from 2 to 4 leads to decrease the surface area of WAC. The surface area is a maximum value (1156 m<sup>2</sup>/g) at the temperature of 700 °C with ZnCl<sub>2</sub> activation in which impregnation ratio is 2/1, but the surface areas (1121 and 1098 m<sup>2</sup>/g respectively) of WAC carbonized at 600 °C with impregnation ratio of 2/1 and 3/1 are quite close to each other. The difference of these surface areas obtained at 600 and 700 °C is about 50 m<sup>2</sup>/g. Therefore, WACs carbonized at 600 and 700 °C were analyzed in depth.

#### 3.3. Influence of chemical impregnation ratio and temperature on the pore volume

The influences of impregnation ratio on the micropore and mesopore volumes of prepared activated carbon at 600 and 700 °C are shown in Fig. 2a and b respectively. These figures indicate that the mesopores are well developed in the activated carbons prepared in this study. The effect of ZnCl<sub>2</sub> on the formations of micropore and mesopore can be understood with

**Table 1** The surface area values (m<sup>2</sup>/g) of WACs prepared at different carbonization temperature and impregnation ratios, and carbonization time.

	Temperature (°C)				
	400	500	600	700	800
<b>30 (min)</b>					
ZnCl <sub>2</sub> /dWR					
1/2	79	114	143	150	98
1/1	108	138	172	174	124
2/1	115	142	185	180	135
3/1	104	134	180	171	115
4/1	52	76	124	130	64
<b>90 (min)</b>					
ZnCl <sub>2</sub> /dWR					
1/2	184	201	226	238	194
1/1	206	234	265	277	213
2/1	218	257	298	299	232
3/1	211	238	286	275	226
4/1	165	195	189	195	173
<b>120 (min)</b>					
ZnCl <sub>2</sub> /dWR					
1/2	200	196	219	224	174
1/1	285	227	259	267	207
2/1	294	235	279	282	214
3/1	278	224	263	265	204
4/1	245	171	187	189	153

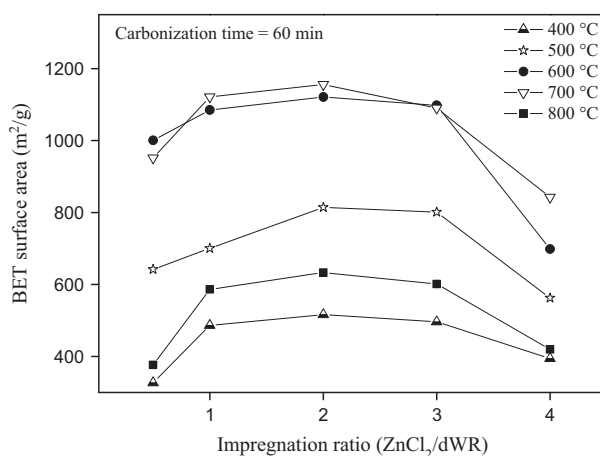


**Figure 1** Influences of carbonization temperature and impregnation ratio on the surface area of prepared WACs.

two competing mechanisms – micropore formation and pore widening (Rodríguez-Reinoso and Molina-Sabio, 1992). At low  $\text{ZnCl}_2$ -to-dWR, micropore formation is dominating mechanism and pore widening becomes important as the ratio increases at 600 °C. Therefore, mesopore volume increases until the impregnation ratio of 3/1. Then, the total pore volume decreases at the impregnation ratio of 4/1. For the total pore volume, similar trend is observed in Fig. 2b indicating the carbonization temperature of 700 °C. Total pore volume increases until the impregnation ratio of 3/1, and then, decreases at the impregnation ratio of 4/1. Furthermore, it is obvious that increasing carbonization temperature from 600 to 700 °C does not change the total pore volume (micropore volume + mesopore volume) substantially, but it causes the micropore volume to decrease. In Fig. 2b, the maximal value of the total pore volume of WAC prepared with impregnation ratio of 3/1 at 700 °C is found to be 0.95  $\text{cm}^3/\text{g}$ , and the total volume of WAC with impregnation ratio of 2/1 at 700 °C is 0.91  $\text{cm}^3/\text{g}$ . The difference between these pore volumes, i.e., 0.95 and 0.91  $\text{cm}^3/\text{g}$  may be negligible, but the maximal value of the total pore volume of WAC prepared impregnation ratio of 3/1 at 600 °C is 1.41  $\text{cm}^3/\text{g}$ . Although the surface areas of

WACs carbonized at 600 and 700 °C with impregnation ratio of 2/1 and 3/1 were determined to be close to each other, the pore volume of WAC prepared impregnation ratio of 3/1 at 600 °C was calculated as a high value which was more than the others, with the difference of about 50%.

Table 3 represents the average pore diameters (4V/A by BET) of WACs produced with the different impregnation ratios at 400–800 °C. As the impregnation ratio was raised for all WACs produced at 400–800 °C, the average pore diameter increased until the impregnation ratio of 3/1, but the average pore diameter decreased when the impregnation ratio becomes 4/1. The maximal value of the average pore diameter was determined to be 5.12 nm for WAC with the impregnation ratio of 3/1 at 600 °C.

### 3.4. Nitrogen adsorption–desorption isotherms

The physisorption isotherms have been classified into six different types by the International Union of Pure and Applied Chemistry (IUPAC) (Sing, 1985). As shown in Figs. 3 and 4,  $\text{N}_2$  adsorption–desorption isotherms of WACs prepared with different impregnation ratios at 600 and 700 °C fit the mixture of type I and type IV with hysteresis loops. Hysteresis loops indicate that WACs have mesoporous, and WACs with narrower hysteresis loops have less mesoporous. The hysteresis loop of WAC prepared with impregnation ratio of 3/1 at 600 °C is the largest compared to the others. It means that WAC prepared with impregnation ratio of 3/1 at 600 °C has the highest mesoporous, and the shape of isotherm of WAC prepared with impregnation ratio of 3/1 at 600 °C resembles type IV. These findings were consistent with the pore volume of WAC prepared impregnation ratio of 3/1 at 600 °C, as shown in Fig. 2a.

### 3.5. FTIR spectra of dWR and WAC

FTIR spectra of WAC prepared at different conditions were determined to be similar. For this reason, only dWR and WAC spectra were compared in Fig. 5. At the spectrum of dWR, the broad absorption band between 3200 and 3400  $\text{cm}^{-1}$  shows the existences of OH groups and the vibration of N–H stretching (Dağdelen et al., 2014). The bands located at 2923 and 2854  $\text{cm}^{-1}$  indicate C–H vibrations in methylene and methyl groups (Sun and Webley, 2010). The band at 1734  $\text{cm}^{-1}$  indicates carbonyl C=O groups. The band located at 1634  $\text{cm}^{-1}$  corresponds to olefinic C=C stretching (Yu and Luo, 2014). The bands at around 1415 and 1365  $\text{cm}^{-1}$  are due to the C–H in-plane bending vibrations in methyl and methylene groups (Yang and Qiu, 2010). The bands located at 1236  $\text{cm}^{-1}$  and an intense band at approximately

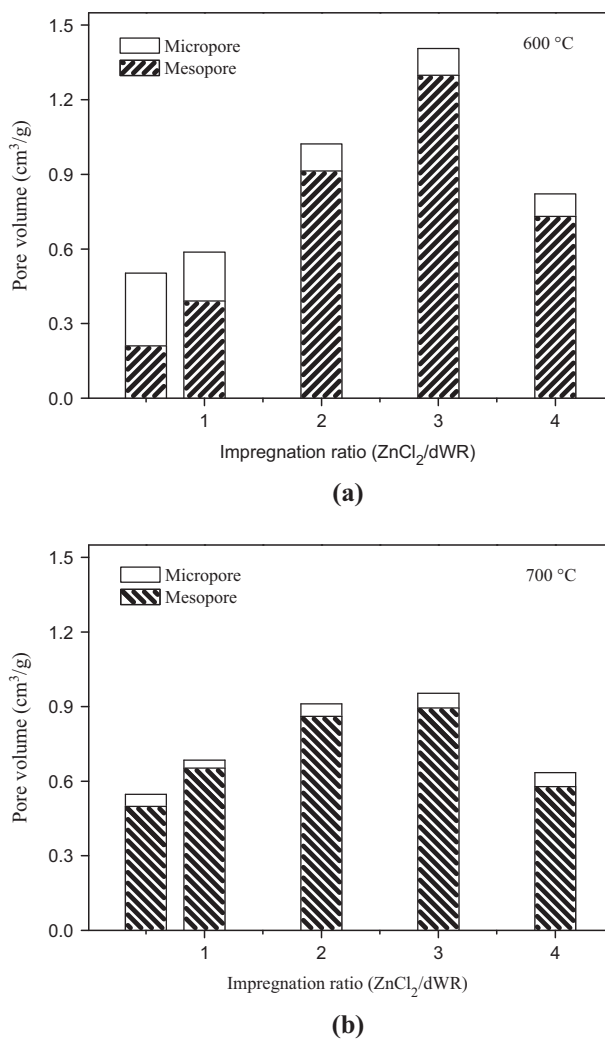


**Figure 2** Influences of impregnation ratio on the micropore and mesopore volumes of prepared WACs at (a) 600 and (b) 700 °C.

**Table 3** Average pore diameter (nm) (4V/A by BET).

$\text{ZnCl}_2/\text{dWR}$	Temperature (°C)				
	400	500	600	700	800
0.5/1	2.00	2.00	2.01	2.30	2.32
1/1	2.17	2.46	2.17	2.44	2.82
2/1	2.21	3.00	3.65	3.15	2.91
3/1	2.46	4.21	5.12	3.50	3.20
4/1	2.36	3.66	4.70	3.01	2.95

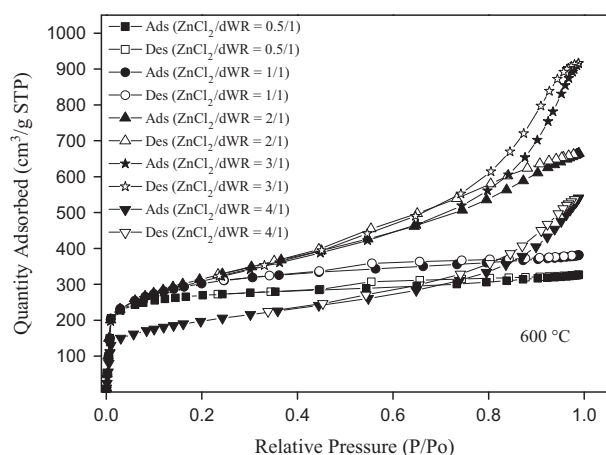


**Figure 3**  $N_2$  adsorption–desorption isotherms of WACs prepared for different impregnation ratios ( $ZnCl_2/dWR$ ) at  $600\text{ }^\circ\text{C}$ .

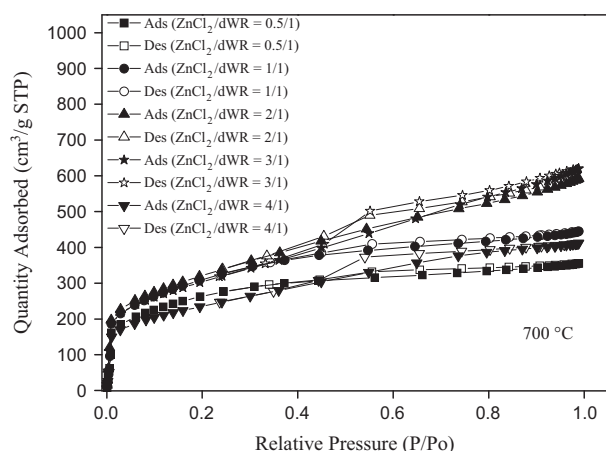


**Figure 4**  $N_2$  adsorption–desorption isotherms of WACs prepared for different impregnation ratios ( $ZnCl_2/dWR$ ) at  $700\text{ }^\circ\text{C}$ .

$1027\text{ cm}^{-1}$  belong to C–O stretching vibrations in alcohols, phenols, or ether or ester groups (Hesas et al., 2013). WAC spectrum has less adsorption bands than dWR spectrum. This indicates that various functional groups present in dWR spectrum disappeared after the carbonization and activation steps. Similar to dWR spectrum, WAC spectrum exhibited the bands between  $1260$  and  $1050\text{ cm}^{-1}$  are attributed to C–O stretching in carboxyl acids, alcohols, phenols and esters (Martins et al., 2015).

### 3.6. Point of zero charge and Boehm titration

The value at which pH (ultimate) is equal to pH (initial) was accepted to be  $pH_{ZPC}$ , and the charge surface is neutral at this pH value. The  $pH_{ZPC}$  of an adsorbent is a fundamental characteristic to comprehend interfacial properties. Moreover, the  $pH_{ZPC}$  of an adsorbent helps to deduce which ionic species can be adsorbed by the activated carbon at desired pH. The value of  $pH_{ZPC}$  of WACs produced at  $600$  and  $700\text{ }^\circ\text{C}$  was determined to be  $5.45$ . The surface of WAC is positively

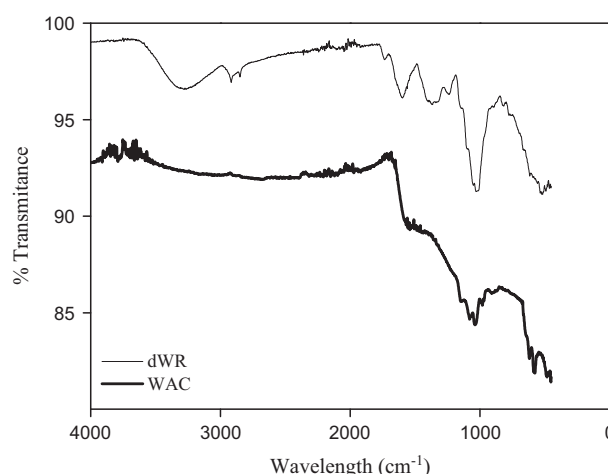


**Figure 5** FTIR images of dWR and WAC.

charged at the pHs below  $5.45$ , while it is negatively charged at pHs above  $5.45$ . Thus, it is predicted that the adsorption of ionic species with positively charged by WAC will be proper at pHs above  $5.45$ . On the other hand, the adsorption of ionic species with negatively charged by WAC will be appropriate at pHs below  $5.45$  because of electrostatic interactions.

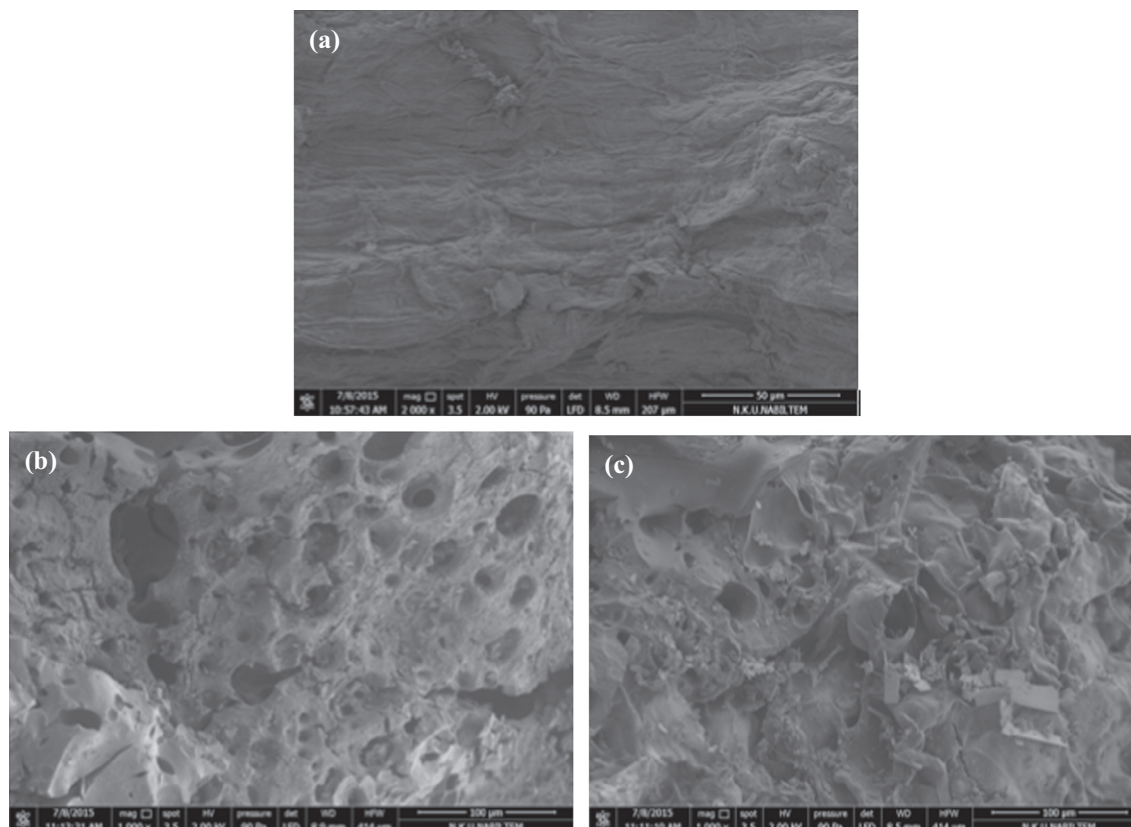
As shown in Table 4, increasing carbonization temperature (at the impregnation ratios of  $3/1$  and  $2/1$  for WACs carbonized at  $600$  and  $700\text{ }^\circ\text{C}$ , respectively) reduces the amount of acidic functional groups and increases the basic surface groups of WAC. The increase in carbonization temperature will make some functional groups decompose to form CO and  $CO_2$ . This is caused by the instability of acidic groups at high temperatures (Boehm, 1994). On the contrary, basic groups are increased when the temperature is increased. These groups can be formed during the cooling of WAC after the carbonization process. This cooling process makes possible to be the fixation of oxygen in the active sites (Boehm, 1994). Similar result was also obtained by Prahas et al. for phosphoric acid activated jackfruit peel waste (Prahas et al., 2008). Furthermore, the result of point of zero charge ( $pH_{pzc} = 5.45$ ) is consistent with Boehm titration results, which explains the dominance of acidic groups on the surface of WACs.

### 3.7. SEM observation of dWR and WAC

The SEM images of dWR at the operating condition with  $2000\times$  magnification and WACs at the operating condition with  $1000\times$  magnification are presented in Fig. 6(a–c). SEM image of dWR in Fig. 6a shows that dWR has smooth surface without distinctive pores. In Fig. 6b, SEM image of activated carbons prepared by using  $ZnCl_2$  chemical activation with impregnation ratio of  $3/1$  at  $600\text{ }^\circ\text{C}$  illustrates an irregular and heterogeneous surface morphology with a well-developed porous structure in various sizes. Moreover, in Fig. 6c, SEM image of activated carbons prepared by using  $ZnCl_2$  chemical activation with impregnation ratio of  $2/1$  at  $700\text{ }^\circ\text{C}$  is similar to Fig. 6b, but there are fewer holes in Fig. 6c than in Fig. 6b. This result supports that WAC prepared by using  $ZnCl_2$  chemical activation with impregnation ratio of  $3/1$  at  $600\text{ }^\circ\text{C}$  has the highest pore volume compared to the other WACs, see Fig. 2.

**Table 4** Results of Boehm titration (molecules/nm<sup>2</sup>).

Sample	Carboxylic	Lactonic	Phenolic	Acidic	Basic	All groups
WAC-600	0.756	0.346	0.402	1.504	0.268	1.772
WAC-700	0.574	0.261	0.209	1.044	0.313	1.357

**Figure 6** SEM images of (a) dWR and WACs carbonized at (b) 600 and (c) 700 °C.

#### 4. Conclusions

The following conclusion can be drawn:

- The resultant activated carbon prepared from biowaste watermelon rind by using zinc chloride with the impregnation ratio of 3/1 at 600 °C has the highest mesopore volume of 1.41 cm<sup>3</sup>/g, which can be used to adsorb molecules with high volumes; dyes, etc.
- WAC produced at 2/1 at 700 °C has the highest surface area of 1156 m<sup>2</sup>/g.
- N<sub>2</sub> adsorption/desorption isotherms fit the mixture of type I and type IV. Additionally, more mesoporosity is present in WACs carbonized at 600 °C with a hysteresis loop type H4, compared to WACs carbonized at 700 °C.

#### Acknowledgment

We gratefully acknowledge the financial support of Trakya University Research Fund under the project number of TÜBAP 2014/130.

#### References

- Açıkyıldız, M., Gürses, A., Karaca, S., 2014. Preparation and characterization of activated carbon from plant wastes with chemical activation. *Micropor. Mesopor. Mater.* 198, 45–49.
- Ai, N., Zeng, G., Zhou, H., He, Y., 2013. Co-production of activated carbon and bio-oil from agricultural residues by molten salt pyrolysis. *Bioresources* 8, 1551–1562.
- Boehm, H.P., 1966. Chemical identification of surface groups. In: Eley, D.D., Pines, H., Weisz, P.B. (Eds.), *Advances in Catalysis*, vol. 16. Academic Press, New York, pp. 179–274.
- Boehm, H.P., 1994. Some aspects of the surface chemistry of carbon blacks and other carbons. *Carbon* 32, 759–769.
- Calvillo, L., Lázaro, M.J., García-Bordejé, E., Moliner, R., Cabot, P. L., Esparbé, I., Pastor, E., Quintana, J.J., 2007. Platinum supported on functionalized ordered mesoporous carbon as electrocatalyst for direct methanol fuel cells. *J. Power Sources* 169, 59–64.
- Dai, Y., Jiang, H., Hu, Y., Fu, Y., Li, C., 2014. Controlled synthesis of ultrathin hollow mesoporous carbon nanospheres for supercapacitor applications. *Ind. Eng. Chem. Res.* 53, 3125–3130.

- Dağdelen, S., Acemioglu, B., Baran, E., Koçer, O., 2014. Removal of remozal brilliant blue R from aqueous solution by pirina pretreated with nitric acid and commercial activated carbon. *Water Air Soil Pollut.* 1899, 1–15.
- Daud, W.M.A.W., Ali, W.S.W., 2004. Comparison on pore development of activated carbon produced from palm shell and coconut shell. *Bioresour. Technol.* 93, 63–69.
- Donald, J., Ohtsuka, Y., Xu, C.C., 2011. Effects of activation agents and intrinsic minerals on pore development in activated carbons derived from a Canadian peat. *Mater. Lett.* 65, 744–747.
- Gonzalez, J.F., Roman, S., Encinar, J.M., Martinez, G., 2009. Pyrolysis of various biomass residues and char utilization for the production of activated carbons. *J. Anal. Appl. Pyrol.* 85, 134–141.
- Hayashi, J., Kazehaya, A., Muroyama, K., Watkinson, A.P., 2000. Preparation of activated carbon from lignin by chemical activation. *Carbon* 38, 1873–1878.
- Hesas, R.H., Niya, A.A., Daud, W.M.A.W., Sahu, J.N., 2013. Preparation of granular activated carbon from oil palm shell by microwave-induced chemical activation: optimization using surface response methodology. *Chem. Eng. Res. Des.* 91, 2447–2456.
- Köseoglu, E., Akmil-Başar, C., 2015. Preparation, structural evaluation and adsorptive properties of activated carbon from agricultural waste biomass. *Adv. Powder Technol.* 26, 811–818.
- Lowell, S., Shields, J.E., 1991. *Powder Surface Area and Porosity*, third ed. Chapman & Hall, London.
- Martins, A.C., Pezoti, O., Cazetta, A.L., Bedin, K.C., Yamazaki, D.A. S., Bandoch, G.F.G., Asefa, T., Visentainer, J.V., Almeida, V.C., 2015. Removal of tetracycline by NaOH-activated carbon produced from macadamia nut shells: kinetic and equilibrium studies. *Chem. Eng. J.* 260, 291–299.
- Milonjić, S.K., Ruvarac, A.L., Šušić, M.V., 1975. The heat of immersion of natural magnetite in aqueous solutions. *Thermochim. Acta* 11, 261–266.
- Okman, I., Karagöz, S., Tay, T., Erdem, M., 2014. Activated carbons from grape seeds by chemical activation with potassium carbonate and potassium hydroxide. *Appl. Surf. Sci.* 293, 138–142.
- Prahas, D., Kartika, Y., Indraswati, N., Ismadji, S., 2008. Activated carbon from jackfruit peel waste by H<sub>3</sub>PO<sub>4</sub> chemical activation: pore structure and surface chemistry characterization. *Chem. Eng. J.* 140, 32–42.
- Qin, C., Chen, Y., Gao, J., 2014. Manufacture and characterization of activated carbon from marigold straw (*Tagetes erecta* L.) by H<sub>3</sub>PO<sub>4</sub> chemical activation. *Mater. Lett.* 135, 123–126.
- Rodriguez-Reinoso, F., Molina-Sabio, M., 1992. Activated carbons from lignocellulosic materials by chemical and/or physical activation: an overview. *Carbon* 30, 1111–1118.
- Ryoo, R., Joo, S.H., Kruk, M., Jaroniec, M., 2001. Ordered mesoporous carbons. *Adv. Mater.* 13, 677–681.
- Saygılı, H., Güzel, F., Önal, Y., 2015. Conversion of grape industrial processing waste to activated carbon sorbent and its performance in cationic and anionic dyes adsorption. *J. Clean. Prod.* 93, 84–93.
- Sing, K.S.W., 1985. Reporting physisorption data for gas/solid systems with special reference to the determination of surface area and porosity (recommendations 1984). *Pure Appl. Chem.* 603.
- Sun, Y., Webley, P.A., 2010. Preparation of activated carbons from corncob with large specific surface area by a variety of chemical activators and their application in gas storage. *Chem. Eng. J.* 162, 883–892.
- Talapaneni, S.N., Mane, G.P., Mano, A., Anand, C., Dhawale, D.S., Mori, T., Vinu, A., 2012. Synthesis of nitrogen-rich mesoporous carbon nitride with tunable pores, band gaps and nitrogen content from a single aminoguanidine precursor. *ChemSusChem.* 5, 700–708.
- Yagub, M.T., Sen, T.K., Afroze, S., Ang, H.M., 2014. Dyes and its removal from aqueous solution by adsorption: a review. *Adv. Colloid Interface Sci.* 209, 172–184.
- Yahya, A.Y., Al-Qodah, Z., Zanariah Ngah, C.W., 2015. Agricultural bio-mass materials as potential sustainable precursors used for activated carbon production: a review. *Renew. Sustain. Energy Rev.* 46, 218–235.
- Yang, J., Qiu, K., 2010. Preparation of activated carbon from walnut shell via vacuum chemical activation and their application for methylene blue removal. *Chem. Eng. J.* 165, 209–217.
- Yu, L., Luo, Y.-m., 2014. The adsorption mechanism of anionic and cationic dyes by Jerusalem artichoke stalk-based mesoporous activated carbon. *J. Environ. Chem. Eng.* 2, 220–229.
- Zhuang, X., Wan, Y., Feng, C., Shen, Y., Zhao, D., 2009. Highly efficient adsorption of bulky dye molecules in wastewater on ordered mesoporous carbons. *Chem. Mater.* 21, 706–716.